JOURNAL OF RESEARCH of the National Bureau of Standards—D. Radio Propagation
Vol. 64D, No. 5, September–October 1960

ELF Electric Fields From Thunderstorms[1, 2]

A. D. Watt

(April 28, 1960; revised May 6, 1960)

The varying electromagnetic fields produced by thunderstorms and associated lightning discharges are examined. Calculated field variations produced by an assumed typical cloud to ground discharge model are found to agree well with observed fields. The magnitude of these vertical electric field changes are observed to decrease very slowly with distance from the source for values comparable to discharge channel heights. From 4 to 20 kilometers a $1/d^3$ relation is observed, and beyond 30 kilometers the field variations appear to follow a $1/d$ relation.

The expected radiation field frequency spectra from 1 cycle per second to 100 kilocycles per second are calculated employing models assumed to be typical of "long" and "short" discharges. The radiation spectra obtained from 1 to 100 kilocycles per second for observed cloud to ground discharge field variations normalized to 1 kilometer are seen to agree within expected limits with calculated values.

The models employed indicate that below 300 cycles per second "long" discharges produce much more energy than "short" discharges, and that inter- and intra-cloud discharges may produce as much energy as cloud to ground discharges.

Anticipated variations of total vertical electric field frequency spectra as a function of distance, based on the work of Wait, are shown for the frequency range from 1 cycle per second to 100 kilocycles per second.

1. Introduction

It is well known that the natural background radio noise field in the region from 3 kc/s to 30 Mc/s is largely produced by lightning discharges. Although the natural noise level above 30 Mc/s is largely due to cosmic sources, Atlas [1] [3] has shown that lightning sources are observable at frequencies as high as 3,000 Mc/s.

Below 3 kc/s, the noise spectra produced by lightning discharges is not well known, although it is generally believed that below 1 c/s the background noise fields are produced largely by ionospheric currents or extraterrestrial sources rather than by lightning discharges.

In view of the somewhat limited information available regarding the ELF electromagnetic fields produced by thunderstorm and lightning activity, it is the purpose of this paper to consider the mechanism by which time varying electric and magnetic fields and their associated frequency spectra are likely to be produced by thunderstorms and lightning discharges.

2. Observed Vertical Electric Field Variations

The vertical electric field at the surface of the earth has a fair weather field potential of approximately 100 v/m with a diurnal variation, which appears to be well correlated with worldwide thunderstorm activity, having approximate plus or minus 20 percent variation about this mean value, as shown by Pierce [2]. The fair weather field is negative since the potential increases with height above the surface of the earth.[4] This means that a vertical rod antenna will have a positive potential with respect to ground.

During a thunderstorm or disturbed weather, the vertical electric field in the vicinity of such a storm can become quite great and usually changes sign from the negative fair weather field to a positive value which, as has been shown by Smith [4], can become quite large, i.e., values in the order of 4,000 v/m. These changes in the vertical electric field caused by motion of clouds and charged volumes are at a relatively slow rate. The magnitude of the change is, however, great and the possible contribution by this mechanism to the total observed vertical electric field spectrum must be considered for frequencies in the order of several cycles per second.

Tamura [5] has observed that, even with thunderstorms 10 to 20 km from the observing point, the field intensity can become several hundred volts positive. In some cases the field slowly varies to a relatively large negative value, although the general trend during storms is for a positive field with rather abrupt negative direction changes during cloud to ground lightning discharges. These negative field changes soon recover (in about a minute) to an average positive field of several hundred volts per meter. The general mechanism involved in a typical cloud to ground discharge can be seen from figure 1

[1] Contribution from Central Radio Propagation Laboratory, National Bureau of Standards, Boulder, Colo.; paper presented at Conference on the Propagation of ELF Radio Waves, Boulder, Colo., Jan. 26, 1960.

[2] The studies contained in this paper were sponsored by the Office of Naval Research under contract NR 371-291.

[3] Figures in brackets indicate the literature references at the end of this paper.

[4] Since $E=-dv/dz$, the vertical electric field considering up in a positive sense is actually a negative quantity as shown by Clark [3]. Considerable care must be taken when reading the literature on atmospheric electricity. Most workers have plotted observed potential gradient which is sometimes referred to as the observed field without the appropriate change in sign.

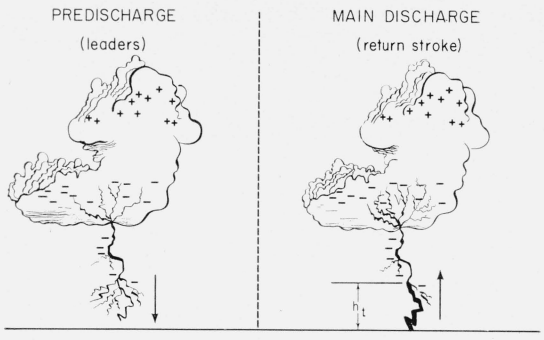

FIGURE 1. *Lightning discharge.*

(a) Predischarge (leaders), $v_l \approx 80$ m/μsec. (during each step), $I_l \approx 300$ amp (avg) (b) Main discharge (return stroke), $v_r \approx 80$ m/μsec., $I_r \approx 30$ kiloamp (avg peak value).

where it is apparent that the negative charge on the bottom of the cloud will produce a positive electric field beneath it. The buildup of charge in the thunderstorm cloud cell produces an increase in potential gradient. When this gradient exceeds the break down potential of the air, the step leader is initiated along a path which generally follows the direction of maximum gradient. Although the instantaneous direction may be quite variable and can contain various "false start" trials as shown, the general trend must be to the ground for this type of discharge. The process of the leader or pilot streamer as it advances in spurts of 10 to 100 m has been described in detail by Schonland [6], and the total period during which it is progressing downward in a cloud to ground discharge can vary appreciably about some average value in the order of 500 to 1,000 μsec.

It is apparent from figure 1 that if the point of observation is beneath the cloud cell in which the lightning discharge is forming that the field will increase positively as the leader lowers negative charge. It is well known that the leader mechanism contributes appreciably to the spectrum of the electric field at frequencies above 20 kc/s [7]; however, aside from the contribution due to the positive field increase during formation and those cases where the leader lowers a substantial part of the total charge, the leader mechanism is not likely to appreciably contribute to the spectrum below about 5 kc/s.

3. Return Stroke Current Moment Characteristics

Once the step leader reaches the earth's surface, the main return stroke is initiated which travels upward with an initial velocity in the order of 80 m/μsec. It should be observed that this vertical upward travel which actually slows down at higher altitudes is really a growth vertically in the downward acceleration of negative charge (in almost all cloud to ground strokes) which has been deposited during the leader process of the lightning discharge. This downward flow of negative charge causes a positive [5] (upward) vertical electric current. Employing well-known concepts, we see that the main return stroke in practically all cases constitutes a positive vertical electric moment which can be obtained by integrating the current times differential height along the discharge path.

The height of various discharge paths differ appreciably, and it is obvious when one visualizes the mechanism involved that the shape of the moment curve as a function of time as well as the relative amounts of vertical and horizontal moment will vary appreciably from one discharge to another. A typical base current versus time for a single stroke is shown in figure 2a. Figure 2b shows the manner in which the return stroke length varies with time, and the effective vertical moment and its differential and integral as a function of time are shown in figure 2c.

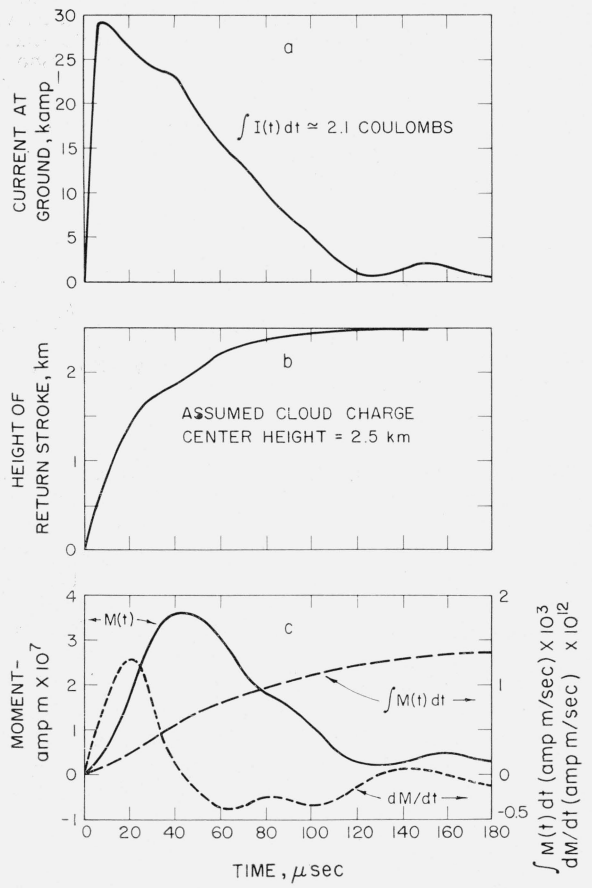

FIGURE 2. *Cloud to ground lightning stroke—estimated median characteristics.*

4. Electric and Magnetic Fields Produced by a Time Varying Vertical Current

A vertical electric monopole on the surface of a flat perfectly conducting earth as shown in figure 3

[5] Schonland, Hodges, and Collens [8] observed only one apparent negative current in more than 350 cloud to ground discharges.

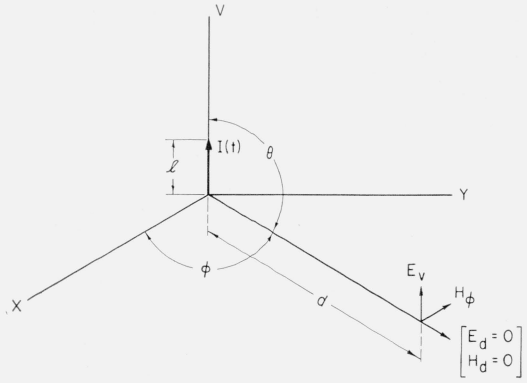

FIGURE 3. *Current monopole field geometry.*

produces both electric and magnetic fields which, on the surface neglecting ionospheric effects, can be written as [6]

$$E_v=\frac{-1}{2\pi\epsilon_0}\left[\int\frac{M(t')\mathrm{d}t}{d^3}+\frac{M(t')}{cd^2}+\frac{dM(t')/dt}{c^2d}\right] \tag{1}$$

(electrostatic) (induction) (radiation)

$$H_\phi=\frac{1}{2\pi}\left[\frac{M(t')}{d^2}+\frac{dM(t')/dt}{cd}\right] \tag{2}$$

(induction) (radiation)

where:

E_v[7] is the vertical electric field in volts/meter,
H_ϕ is the tangential magnetic field in ampere turns/meter,
ϵ_0 is the permittivity of free space $=[36\pi\times10^9]^{-1}$ in farads/meter,
$M(t)$[8] is the changing vertical electric moment, $I\times l$, in ampere meters,
$I(t)$ is the dipole antenna current in amperes,
l is the dipole length in meters,
d is the distance from the source to the point of observation in meters where $d>>l$,
c is the velocity of light $=3\times10^8$ m/sec, and
t' $=(t-d/c)$.

If the current is chosen as $I(t)=I\cos\omega t$, we can write

$$E_v=\frac{-Il}{2\pi\epsilon_0}\left[\frac{\sin\omega t'}{\omega d^3}+\frac{\cos\omega t'}{cd^2}-\frac{\omega\sin\omega t'}{c^2d}\right] \tag{3}$$

and

$$H_\phi=\frac{Il}{2\pi}\left[\frac{\cos\omega t'}{d^2}-\frac{\omega\sin\omega t'}{cd}\right]. \tag{4}$$

It is interesting to observe the effects of distance upon the various terms of the electric field produced by an oscillating electric dipole [11]. Beyond one wavelength E_v and H_ϕ decay as $1/d$. In figure 4, obtained from Norton, it can be seen that between $d/\lambda=0.1$ and 1, all three terms are contributing to E_v, while for distances less than 0.1 the $(1/d)^3$ term predominates.

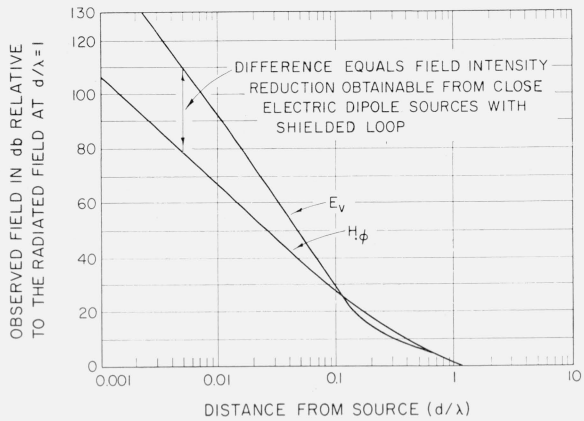

FIGURE 4. *Electric fields versus distance for oscillating electric or magnetic dipoles.*

5. Effective Discharge Moment Field Relations

From eq (1) we obtain the three components for an electric monopole. The radiation field term, E_r, can be shown to be

$$E_r=\frac{-2dM(t')/dt}{10^7d}, \tag{5}$$

the induction field term is

$$E_i=\frac{-60M(t')}{d^2} \tag{6}$$

and the electrostatic term is

$$E_e=\frac{-1.8\times10^{10}\int M(t')\,dt}{d^3}. \tag{7}$$

It should be emphasized that the monopole fields shown hold only as long as d is large compared to the monopole length, and reasonably small compared to the height of the ionosphere whose effects have thus far been neglected.

Before attempting to examine fields produced by actual discharges, it is important to note that the peak currents observed at the ground vary appreciably about the average 30-kamp value shown in figure 2a. Cloud to ground stroke data obtained from Robertson, Lewis, and Faust [12] are shown in figure 5 along with radiated field data from Taylor and Jean [13] where it is seen that the currents have a somewhat greater dynamic range than a Rayleigh

[6] See for example Jordan [9] or Wait [10].
[7] Note that with respect to the conventional spherical coordinates, $E_v=-E\theta$ when $\theta=90°$.
[8] It is noted that $\int_0^\tau M(t)\,dt=q_t\,l_{\mathrm{eff}}$ where q_t is the total charge lowered in coulombs and l_{eff} is the average effective length of the discharge in meters.

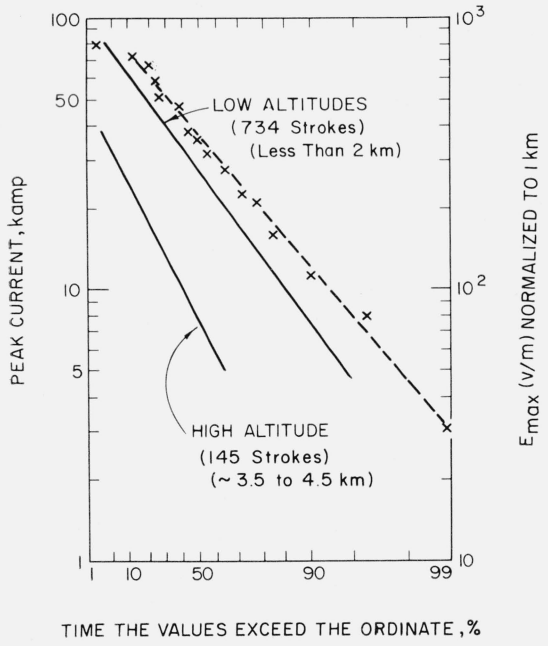

FIGURE 5. *Cumulative distribution of cloud to ground lightning stroke current amplitudes at the earth's surface, and* E_{max} *of radiated waveform normalized to one km.*

——— Peak current from Robertson, Lewis, Faust [12]. ——— Peak fields from Taylor and Jean [13].

distribution which has a slope of (−1) on this graph. It should also be noted that the high altitude strokes have much lower peak current amplitudes which may result from the lower break down potential of air at high altitudes or the lower ground conductivity high in the mountains. The slope of the distribution of normalized peak radiated fields is similar to that for low altitude (below 2 km at the ground) currents as would be expected.

6. Variation With Distance of Field Strength Changes During Lightning Discharges

Observed changes in the vertical electric field near to thunder storms obtained from Hatakeyama [14], Tamura [5], Florman [15], and Taylor and Jean [13] are plotted on figure 6 where it appears that the $1/d^3$ relation is valid for distances of about 4 to 20 km. This agrees with Morrison [16] who indicated that $E_e=E_r$ at $d=26$ km. Beyond 30 km the observed points group around the $1/d$ line with an amount of scatter expected from the variations in peak radiated field.

The peak negative swing of the radiation field assuming a median stroke from figure 5 is seen to be

$$E_r \simeq 300/d(\text{km}). \tag{8}$$

The peak field calculated for the example in figure 2 is $E_r \simeq 260/d(\text{km})$ which would indicate that it is typical of a median return stroke.

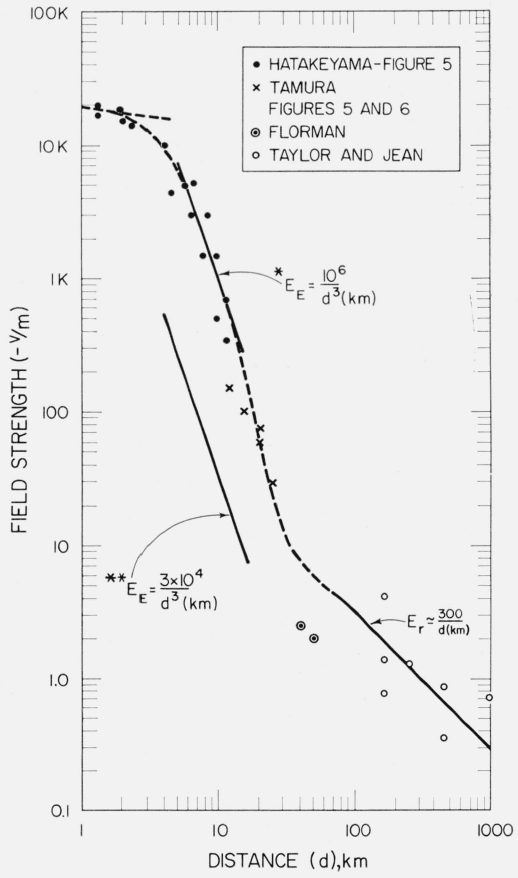

FIGURE 6. *Peak electric field variation from lightning discharges.*

*for a complete discharge, assuming $q\times l=5.6\times10^4$ amp meter sec. **for a single return "short" stroke (current flow from 0 to 150 μsec.)

When the electrostatic term is calculated with eq (7) and a value of $\int M(t')/dt \simeq 1.5\times10^3$ amp meter-seconds, we obtain

$$E_e \simeq 3\times10^4/d^3(\text{km}). \tag{9}$$

(single stroke)

It is obvious that this line shown on figure 6 is far below the observed values. This relation takes into account only the charge lowered during the first 180 μsec which, for the example in figure 2a, is 2.1 coulombs assuming that the current ceased to flow after this time. This assumption, which is allowable for the VLF radiation spectra considerations, is certainly not valid as far as the total electrostatic field change is concerned.

Typical "long"[9] cloud to ground discharges contain several multiple strokes each lasting about 100 μsec and separated by an average time of about 40 millisec. The median peak current is about 30 kamp, and after each stroke a relatively small amount

[9] A long discharge occurs when a small ($I\simeq500-1000$ A) current continues to flow for several hundred milliseconds, and $q_l \geq 10$ coulombs. Short discharges also occur where the current flow stops after about 4 millisec and $q_l\simeq2$ to 10 coulombs.

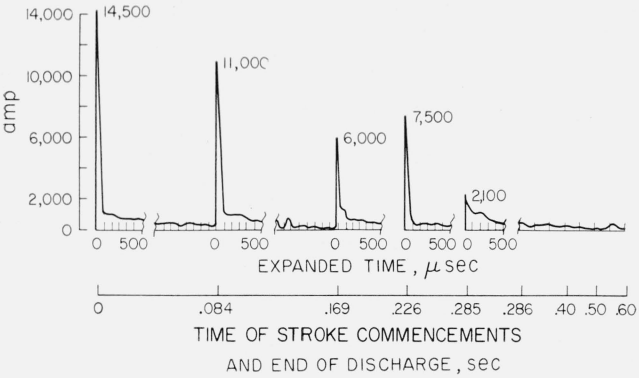

FIGURE 7. *Lightning stroke, complete discharge current.*

Record 208 7-31-42 smokestack of Anaconda Copper Mining Co., Great Falls, Montana (From McCann).

of current (around 500 to 1,000 amp) continues to flow between these strokes. A typical long discharge from McCann [17] is shown in figure 7. Although the peak currents are less than the expected median value, it is instructive to note that 81 coulombs of charge were lowered to the earth in this complete discharge as compared to only 2.1 during the single "short discharge" stroke of figure 2a. This means that a large portion of the charge is actually lowered between and after the main strokes.

Since the change in the electrostatic field is proportional to the charge lowered times the effective height, it is obvious that the actual field change observed for a complete discharge will be much greater than that indicated by (9) for a typical single stroke. It should also be noted that during the high currents of the return stroke, not only is the total charge lowered small, but in addition the effective height is likely less than during the between stroke current flow. The charge of 81 coulombs is larger than the average value of about 10 to 20 shown by McCann [17]. Assuming an average value of 20 coulombs and an average effective height of 2.5 km, we obtain

$$E_e \simeq 10^6/d^3 \text{ (km)} \quad \text{(total discharge)} \tag{10}$$

which is seen from figure 6 to agree very well with observed field changes.[10]

When the field is observed at a distance, comparable or short compared to the discharge length, eq (7) no longer is valid. In close where $d<<l$, it is shown by Wait [10] that the length of the column is no longer a factor. The field is now a function of I and d, and we can write

$$H_\phi = \frac{I}{2\pi d} \tag{11}$$

$$E_v \simeq \frac{\mu\omega I}{\pi^2} \log_e\left(\frac{2\pi d}{\lambda}\right) \tag{12}$$

where μ is the permeability of the medium $= 4\pi\times10^{-7}$h/m for free space, and λ is the free space wavelength in meters. For these relations to hold $d<<l$, and $d/\lambda<<1$. Thus it is seen that the magnitude of E_v will vary slowly with d. For example, if d varies from 4 to 1 km and we assume λ in the order of 6×10^4 km ($f=10$ c/s), the log function varies by about 1 to 1.2. A dotted line with this slope is drawn at the top of figure 6 where it appears that the observed fields are varying in about this manner from 1 to 4 km.

7. Frequency Spectra of Individual Return Strokes

It is instructive to consider the frequency spectrum of an individual return stroke such as shown in figure 2 where the complete event is considered as being consumated in approximately 180 μsec. The frequency spectrum of the induction field term will first be considered because of the ease with which it can be obtained.

The induction field produced, E_i, from eq (6) and figure 2c is seen to be an unidirectional pulse with an area in (v/m). The frequency spectrum of the induction field can be obtained by means of the Fourier transform

$$G(f)_i = \int_{-\infty}^{\infty} E(t)_i e^{-j\omega t} dt$$

$$= \frac{-60}{d^2}\int_{-\infty}^{\infty} M(t') e^{-j\omega t} dt. \tag{13}$$

When the frequency spectrum is obtained from the response of narrow band filters, the relations described in the appendix must be employed.

It is well known [20] that for a pulse of length τ, the frequency spectrum is essentially constant for $f \leq 1/3\tau$ and that $G(f)=A$ where A is the area of the pulse. Since $\tau \simeq 180$ μsec, we can write for the single isolated stroke

$$|G(f)_i| = \frac{60}{d^2}\int_0^{\sigma} M(t')dt \tag{14}$$

$$200 \text{ c/s} \leq f \leq 2{,}000 \text{ c/s}.$$

If $M(t)$ actually became and remained zero beyond 180 μsec, eq (14) would be valid for all frequencies below 2,000 c/s. Since in a typical "long discharge" the channel continues to carry some 500 to 1,000 amp until the next stroke or for a time in the order of a hundred milliseconds, the value of $\int M(t)dt$ given in figure 2c is no longer valid beyond about 20 millisec and a lower limit of around 200 c/s must be placed on f in eq (14).

The radiation spectrum in this frequency range can be obtained by observing from eq (3) that

$$G(f)_r = \frac{2\pi f d G(f)_i}{3\times10^8} \tag{15}$$

[10] This relation obtained from independent data is the same as that given by Pierce [18]. Reference [18] and its companion paper [19] contain a large amount of useful information relative to the characteristics of lightning discharges.

and as a result combining (14) and (15)

$$|G(f)_r|=\frac{4\pi f}{10^7 d}\int_0^\tau M(t)\,dt \tag{16}$$

$$200 \text{ c/s} \leq f \leq 2{,}000 \text{ c/s}.$$

Assuming a typical average value of 1.4×10^3 for $\int M(t)dt$ for the first 180 μsec, we can write

$$|G(f)_r|\simeq\frac{2f}{10^3 d} \tag{17}$$

typical avg long discharge, 200 c/s$\leq f\leq$2,000 c/s;
typical avg short stroke, $f\leq$2,000 c/s.

The spectrum below 100 c/s for a long discharge can be obtained by observing the shape of the $\int M(t)\,dt$ for the complete discharge as shown in figure 8. This function is seen to be essentially a ramp function with a linear slope $m\simeq1.7\times10^6$ amp meters out to the end of the complete discharge which may be in the order of 100 to 500 millisec. From the end of the discharge, the electrostatic field recovers to its initial value in a period of the order of 100 sec.

A ramp function with a slope "m" is known to have a spectrum

$$G(f)=\frac{-m}{4\pi^2 f^2} \tag{18}$$

Combining eq (3), (7), and (18) we obtain

$$|G(f)_r|=\frac{2m}{10^7 d} \tag{19}$$

$$10\leq f\leq 100 \text{ c/s}.$$

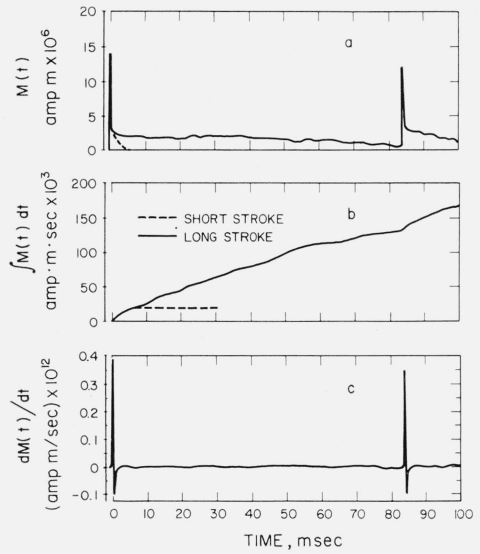

FIGURE 8. *Typical long discharge moment relationships.*

Employing an assumed typical $\int M(t)dt$ with an m of 1.7×10^6 amp meters

$$|G(f)_r|\simeq\frac{0.3}{d} \tag{20}$$

$$10 \leq f\leq 100 \text{ c/s typical avg discharge.}$$

It is interesting to observe that the radiated spectrum in this region is independent of frequency.

For frequencies in the order of 1 c/s, the $\int M(t)dt$ looks like a saw-tooth wave where the important contributions come from the leading edge which approximates a step function. The step function has the well known spectrum

$$G(f)=\frac{h}{2\pi f} \tag{21}$$

where h is the height of the step.

Combining eqs (3), (7), and (21) we obtain

$$|G(f)_r|=\frac{4\pi f}{10^7 d}\int M(t)dt(\max) \tag{22}$$

$$0.2\text{c/s}\leq f\leq 2\text{c/s}.$$

If we employ the maximum moment integral value shown in figure 8 as 1.5×10^5 amp meter seconds, we obtain

$$|G(f)_r|\simeq\frac{0.2f}{d}. \tag{23}$$

The radiation spectrum obtained for an assumed average complete cloud to ground discharge is shown in figure 9 where the straight line sections are obtained from the preceding simplified relationships

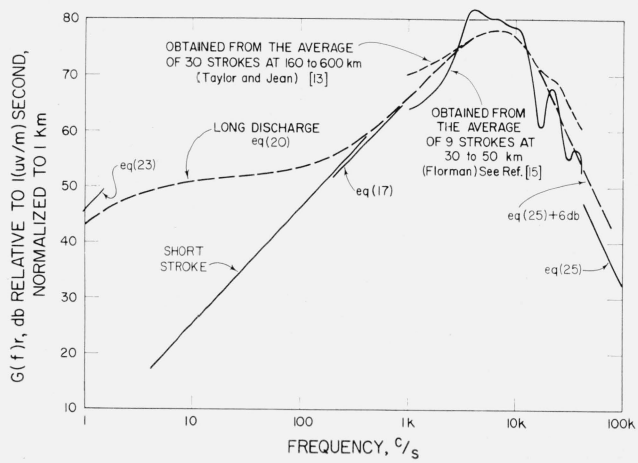

FIGURE 9. *Calculated and observed frequency spectrum of the radiation component of field strength from an average cloud to ground discharge, normalized to a distance of 1 km. (precursor fields have been neglected).*

over the frequency range where they are expected to be valid. The solid and dotted curves represent the average spectra obtained by Fourier transforms of observed fields of individual cloud to ground strokes. The solid straight line with a 12 db/octave slope near 50 kc/s was calculated employing the ramp function transform and the initial slope of the dM/dt curve in figure 2c. The general expression is

$$G(f)_r=\frac{m}{2\pi^2 10^7 f^2 d}. \tag{24}$$

If we employ a slope $m=8\times10^{16}$ amp meters/sec^2

$$G(f)_r=\frac{4\times10^8}{f^2 d} \tag{25}$$

$$f>50 \text{ kc/s}.$$

This line appears to lie about 6 db below the observed spectral values in the 40-kc/s region. If the waveform in figure 2c is closely observed, it is apparent that the reversal in slope at 20 μsec will contribute almost an equal amount to the frequency spectrum in the 30- to 50-kc/s region. Adding 6 db to the values from eq (25) gives good agreement with the observed spectra.

It should be emphasized that individual spectra will vary appreciably since the moment time functions of individual discharges are quite variable. The maximums and minimums observed in the 15- to 40-kc/s region of the radiation spectra obtained from Florman are caused by the different lengths of the+and−half cycles of the moment differential, and each individual discharge is likely to have this type of structure above 15 to 20 kc/s.

The average frequency spectra shown by the dashed lines in figure 9 are based on assumed average cloud to ground discharges where the low frequency portion for the long discharge include the effects of normal multiple strokes. The actual spectrum of any particular cloud to ground discharge may vary appreciably from the spectra shown. There is also a possibility that discharges from tropical types of storms may differ appreciably from the results shown here which are based on a model believed to be fairly typical of the discharges occurring in temperate zone thunderstorms. It is instructive to observe that in the frequency range from roughly 10 to 100 c/s that the radiation spectrum for a long discharge appears to be essentially constant. This results from the appreciable current flow between multiple strokes which may last for periods up to several hundred milliseconds. For short discharges where the current ceases to flow relatively soon after the initial stroke, the frequency spectral components continue to decrease with decrease in frequency as indicated by eq (17). Since the frequency spectrum components in the 1- to 200-c/s region are seen to be primarily generated by the relatively low amplitude current flow between strokes, it would appear that inter- and intracloud strokes with appreciable vertical travel may be as effective as cloud to ground strokes in producing ELF energy. The importance of the initial slope of the dM/dt curve in producing energy in the 3- to 30-kc/s region indicates that cloud to cloud discharges are not likely to produce large VLF fields.

8. Variation of Frequency Spectra With Distance

The frequency spectra shown in figure 9 would not be observable at any given location because of the wide frequency range covered. The actual observed field would vary according to eqs (3) and (4) if the ionosphere could be neglected and the earth were a perfectly conducting flat plane. For distances short compared to the height of the ionosphere, this assumption is relatively valid provided of course that the distance is large compared to the height of the discharge channel.

Wait [21] has treated the waveform variations at short ranges, and also given the relationships anticipated at longer ranges for the observed electric and magnetic fields relative to the plane earth radiation field from calculations based on the waveguide concept [21, 22]. The results obtained are shown in figure 10 in terms of the W function which is the ratio (expressed in decibels) of the vertical electric field to the radiation component of the vertical electric field for an assumed infinitely conducting plane. The frequency spectra expected at 10 and 100 km from a typical average discharge have been calculated with the aid of figures 9 and 10 and the results shown in figure 11. For longer ranges the appropriate W function values can be obtained from Wait [21 to 23].

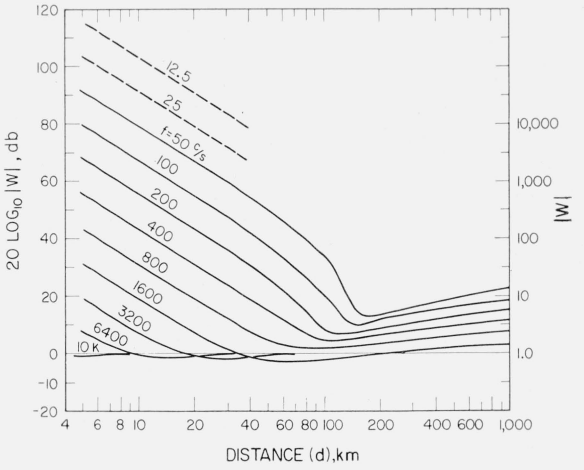

FIGURE 10. *Ratio of actual vertical electric field to the radiation component over an infinitely conducting plane,* $|W|=E_v/E_r$ *(from Wait).*

Calculations based on ionospheric: height=90 km, parameter, $\omega_r=5\times10^5$ rad/sec } night.

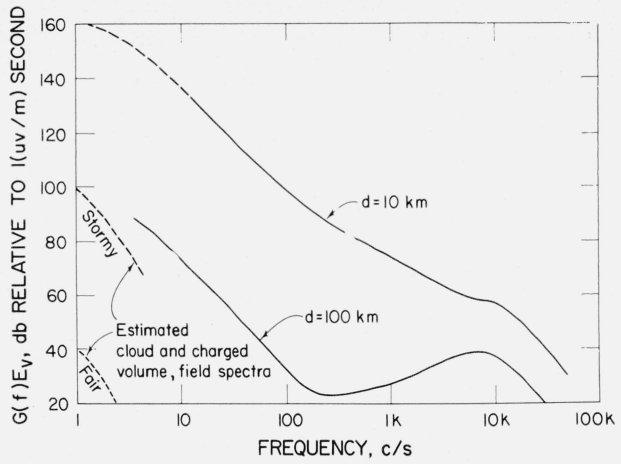

FIGURE 11. *Calculated spectrum of the vertical electric field for an assumed average long discharge cloud to ground lightning discharge,* d *km from the observing point.*

9. Spectra From Fields Produced by Motions of Clouds

The motion of clouds and charged volumes produces relatively large vertical electric field changes. The magnitude and rate of change in these fields suggest that a very rough approximation of the spectra for $f<1$ c/s might be obtained by considering portions of $E_v(t)$ which appear as ramp functions. Typical slopes are in the order of 4 and 0.004 (v/m)/sec for stormy and fair weather fields. Employing eq (18) we obtain

$$G(f)E_v \simeq \frac{1}{10f^2}$$

stormy clouds

$f \simeq 1$ c/s

and

$$G(f)E_v \simeq \frac{1}{10^4 f^2}$$

fair weather

$f \simeq 1$ c/s.

For frequencies above 1 c/s the spectrum is likely to decrease as $1/f^3$ since the field appears not to have discontinuity in slope for $f \geq 1$ c/s. These fields are included in figure 11 to give a rough estimate of possible contributions from this mechanism. Loop antennas will of course be much less subject than whips to effects of this kind.

The author acknowledges the assistance received from: J. R. Wait, E. L. Maxwell, A. G. Jean, and W. L. Taylor during many helpful discussions, as well as permission to use material prepared by them; and from Winifred Mau during the preparation of the manuscript.

10. Appendix. Filter Impulse Response

It should be observed that the frequency spectrum as defined has the dimensions of $E(t)$ multiplied by time which in this case is (volts/meter) seconds. The frequency spectrum amplitude observed with a spectrum analyzer is dependent on the characteristics of the filter employed. The impulse function response of a circuit is given by

$$v_0(t)=\frac{A}{\pi}\int_0^\infty A(\omega)\cos\left[\omega t - B(\omega)\right]d\omega$$

where A is the area of the impulse function, $A(\omega)$ and $B(\omega)$ are the amplitude and phase functions of the circuit. If we assume an idealized loss-less rectangular filter with a linear phase $B(\omega)=S\omega$, the output is

$$v_0(t)=4AF_c\left[\frac{\sin\omega_c\,(t-S)}{\omega_c(t-S)}\right]\cos\omega_0\,(t-S)$$

where the peak transient response is $2Ab$ which means that peak output of this filter is $2bg(\omega)$ provided of course that $g(\omega)$ is constant over the 6-db bandwidth b. In actual practice $A(\omega)$ is not rectangular and the peak response of a physical filter with unity gain at the center frequency is given as

$$\begin{aligned} V_0(\text{peak}) &= kg(\omega)\ b \\ &= kG(f)\ b \end{aligned}$$

where k is dependent on filter configuration, and varies from values of about 1.5 to 3 for typical filters.

11. References

[1] D. Atlas, Radar lightning echoes in atmospherics in vertical cross section, Recent Adv. Atmos. Elec., pp. 441 to 459 (Pergamon Press, Inc., New York, N.Y., 1958).

[2] E. T. Pierce, Some topics in atmospheric electricity, Recent Adv. Atmos. Elec., pp. 5 to 16 (Pergamon Press, Inc., New York, N.Y., 1958).

[3] J. F. Clark, The fair-weather atmospheric electric potential and its gradient, Recent Adv. Atmos. Elec., pp. 61–74 (Pergamon Press, Inc., New York, N.Y., 1958).

[4] L. G. Smith, Electric field studies of Florida thunderstorms, Recent Adv. Atmos. Elec., pp. 299 to 308 (Pergamon Press, Inc., New York, N.Y., 1958).

[5] Y. Tamura, Investigations on the electrical structure of thunderstorms, Recent Adv. Atmos. Elec., pp. 269 to 276 (Pergamon Press, Inc., New York, N.Y., 1958).

[6] B. F. Schonland, The pilot streamer in lightning and the long spark, Proc. Roy. Soc. (London) [**A**] **220,** pp. 25 to 28, (1953).

[7] A. D. Watt and E. L. Maxwell, Characteristics of Atmospheric noise from 1 to 100 kc, Proc. I.R.E. **45,** No. 6, pp. 787 to 794, (1957).

[8] B. F. J. Schonland, D. B. Hodges, H. Collens, Progressive lightning V, A comparison of photographic and electrical studies of the discharge process, Proc. Roy. Soc. (London) [**A**] **166,** pp. 56 to 75 (1938).

[9] E. C. Jordan, Electromagnetic waves in radiating systems (Prentice Hall, Inc., New York, N.Y., 1950).

[10] J. R. Wait, Electromagnetic radiation from cylindrical structures (Pergamon Press, Inc., New York, N.Y., 1959).

[11] J. R. Wait and James Householder, Mixed-path ground-wave propagation: 2. Larger distances, J. Research NBS **59,** 19 (1957) RP2770; also K. A. Norton, private communication.
[12] L. M. Robertson, W. W. Lewis, and C. N. Faust, Lightning investigation at high altitudes in Colorado, Trans. AIEE **61,** pp. 201 to 208 (1942).
[13] W. L. Taylor and A. G. Jean, Very-low-frequency radiation spectra of lightning discharges, J. Research NBS **63D,** pp. 199 to 204 (1959).
[14] H. Hatakeyama, The distribution of the sudden change of electric field on the earth's surface due to lightning discharge, Recent Adv. Atmos. Elec., pp. 269 to 276 (Pergamon Press, Inc., New York, N.Y., 1958).
[15] E. F. Florman, Private communication.
[16] R. B. Morrison, The variation with distance in the range zero-100 km of atmospheric wave-forms, Phil. Mag. **44,** pp. 980 to 986 (1953).
[17] G. D. McCann, The measurement of lightning current in direct strokes, Trans AIEE **63,** pp. 1157 to 1164 (1944).
[18] E. T. Pierce, Electrostatic field-changes due to lightning discharges, J. Roy. Met. Soc. **81,** 229 (1955).
[19] E. T. Pierce, The development of the lightning discharge, J. Roy. Met. Soc. **81,** pp. 229 to 240 (1955).
[20] Reference Data for Radio Engineers, Intern. Telephone and Telegraph Corp., p. 1012 (1956).
[21] J. R. Wait, On the waveform of a radio atmospheric at short ranges, Proc. I.R.E. **44,** No. 8, p. 1052 (1956).
[22] J. R. Wait, Mode theory and the propagation of ELF radio waves, J. Research NBS **64D,** 387 (July 1960).
[23] J. R. Wait and N. F. Carter, Field strength calculations for ELF radio waves, NBS Tech. Note 52 (March 1960).

(Paper 64D5–77)

551273—60——2